Design and evaluation of Ti-15Mo-2Fe alloy for biomedical applications based on electronic parameters

Nthabiseng Abigail Moshokoa[1*], *Lerato* Raganya[2], *Nkutwane Washington* Makoana[3], *Maje* Phasha[4] and *Mamookho Elizabeth* Makhatha[1]

[1]Department of Metallurgy, School of Mining and Metallurgy and Chemical Engineering, University of Johannesburg, Doornfontein Campus, Johannesburg, South Africa.
[2]Advance Materials Engineering, Manufacturing Cluster, Council for Scientific and Industrial Research, Meiring Naude Road, Brummeria, Pretoria 0184, South Africa.
[3]National Laser Center, Council for Scientific and Industrial Research, Meiring Naude Road, Brummeria Pretoria 0184, South Africa.
[4]Physical Metallurgy Group, Advanced Materials Division, Mintek, 200 Malibongwe Drive, Randburg 2125, South Africa.

Abstract. Metastable β-Ti alloys that are evaluated using various electronic parameters to predict their phases and deformation products are gaining much research attention, especially in the biomedical application space. The aim on this study is to evaluate the influence of phase and deformation mechanism on the compression properties of Ti-15Mo-2Fe wt.% alloy designed using electronic parameters such as the B_0-M_d, and the Mo_{eq} methods. Phase evolution and deformation mechanism were experimentally evaluated before and after compression test using X-ray diffraction, and Optical Microscope. The XRD patterns before and after compression illustrated the presence of α″, "R" and β phases. OM micrograph demonstrated β equiaxed grains only before compression and wide deformation bands and slip lines that could be related to deformation mechanism such as mechanical twins and slip were detected in the Ti-15Mo-2Fe. The alloy exhibited high ultimate compressive strength of 1522 MPa, compressive yield of 1088 MPa and compressive strain of 33%. The alloy showed potential to be considered for biomedical applications especially those in vascular stents because of its high strength and % strain.

* Corresponding authors : *Nthabisengmoshokoa@gmail.com, Majep@mintek.co.za, emakhatha@uj.ac.za

1 Introduction

Titanium (Ti) alloys are found in several applications such as biomedical applications, aerospace, marine and chemical environments, because of properties including mechanical strength, fatigue resistance, corrosion resistance and biocompatibility [1] [2], [3]. Metastable β titanium alloys are amongst the various type of Ti alloys and they find their use in biomedical applications due to properties that include high strength, density, ductility, high corrosion resistance and low toxicity, [4], [5]. According to Bahl *et al*., there are categories of biomedical β Ti alloys with their respective specific properties and they are: orthopedic applications that falls under the structural alloys and for cardiovascular orthodontic applications that falls under functional alloys, [6]. Metastable β Ti are processed using different processing techniques such as solution treatment or thermo-mechanical processing and they are characterized for their phase, microstructural constituents and mechanical properties using various methods such as tensile testing and compression test.

Metastable β Ti alloys are continuously being developed using both trial and error method and the electronic structures with the aim of stabilizing the β phase, predicting the deformation mechanisms and improving properties such as strength, elastic modulus using this non-toxic elements and also incorporating low-cost elements such as Fe and Mn [7], [8]. The use of theoretical predictions such as the d-electron method where two parameters such as the average *Bo* and *Md* value proposed by [3], [9], The molybdenum equivalence (*Moeq*) are mostly used instead of the trial and error methods to predict the formation of phases and deformation mechanisms [10]. The development of new metastable β Ti alloys that will depict wide uniform elongation and higher strain hardening rate are widely explored in the current times. Due to the existence of certain phase constituents and different deformation mechanisms which are dependent on the β phase stability, metastable β Ti alloys have become vital amongst the different Ti alloys, [4].

Chemical stability and deformation mechanism of metastable β Ti alloys transforms from stress induced martensitic to mechanical twinning and lastly to dislocation slip with an increase in β phase stability, [4], [11].

Extend of deformation and type of the deformation influence the resulting mechanical property behaviour of the alloy. For example, when the deformation mechanism is composed of only slip then the alloy is said to possess very low ductility, but the yield strength is usually high [12]. Metastable β Ti alloys deformation can be difficult, and they can be related to the stability of β phase and the extent of deformation [13]. It has been reported by Wang *et al.* and Yang *et al.* that when dislocation slip is the dominant deformation mechanism, the material will possess high strain levels, very low ductility but the yield strength will be high [14]. According to Min *et al.* 2010 an alloy where the dominant deformation mechanism is twinning, that alloy is said to exhibit a high strain hardening rate and large ductility, but the yield strength is reported to be low [15].

Bhattacharjee *et al.* and Paradkar *et al.* stated that better combination of strength and ductility can be achieved when an alloy exhibit the existence of stress induced martensitic (SIM) deformation mechanism [12], [16], hence the controlling the deformation mechanism is taken as one of the key strategy that can be used in optimizing mechanical properties in β Ti alloys. Currently, researchers are making significant efforts in understanding and exploring how to control the β phase stability that has an impact in the deformation mechanisms [3], [17] where deformation mechanisms and presence of phases are predicted using theoretical methods as opposed to the trial-and-error method. Sadeghpour *et al.* investigated the compression properties of Ti-Al-Mo-V-Cr alloy after several processing techniques such as cold rolling, where theoretical methods were employed. They reported the stress induced martensite (SIM), twinning and dislocation slip mechanism in the studied alloys, they reported yield strength that ranged from 803-930 MPa and higher fracture strain of 49 % [13].

Another study was conducted on cold rolled Ti-15Mo and Ti-15Mo-1Fe by Min *et al.* designed using the theoretical methods where they reported the highest tensile strength of 837 MPa in Ti-15Mo-1Fe with 19 wt.% elongation and deformation mechanism such as mechanical twinning and slip [15]. Additional research conducted by [18] on as-cast Ti-xTa-xHf-xZr alloys for self expandable stents illustrating high tensile strength and yield strength compared to other metallic stent materials. The high strength in the studied alloys were reported to be influenced by the presence of ω_{ath} phase that was characterised using the TEM technique. [19] developed new Ti-xMo-yFe (x= 8, 9, 10.5 wt.% and y = 0, 1, 2 wt.%) alloys with the purpose of enhancing their strength-ductility trade off and high work hardening rate, as potential candidates for use in balloon expandable stents. Deformation mechanisms such as SIM, {332} <113> mechanical twinning and dislocation slip were observered in those alloys, with the formation of {332} <113> twins reported to be responsible for the high and steady work hardening rate. The Ti-9Mo-1Fe alloy in comparison with other Ti alloys revealed a high yield strength, tensile strength, high elastic modulus but the total elongation was significantly low. Ti-12Mo alloy was the first to be designed for intended use in balloon expandable (BE) stents by [20], [21]. This binary alloy revealed the presence of TWIP and TRIP deformation mechanisms, resulting to a high work hardening rate of 2000 MPa, [11]. [22], UTS of 660 MPa and elongation of 45 %.

Extensive work has been and continues to be published on the metastable β Ti alloys that undergo through different process and characterization techniques that will have potential to be used in biomedical applications. The above literature studies demonstrate that Ti based alloys with different alloying elements such as Fe and Mo are mostly employed for biomedical applications using theoretical predictive methods. However, the current published literature studies shows that there is a still gap to be explored in the influence of phase constituents, deformation products on the mechanical properties of Ti-Mo-Fe alloys with high Mo content and low Fe elements that are subjected to solution treatment and compression test. Therefore, the present study focuses on designing and evaluating low-cost Ti-15Mo-2Fe alloy using electronic parameters such as *Bo-Md* and *Moeq* to forecast phase constituents and deformation products and to investigate the effect of deformation products on the compression properties.

2 Methodology

2.1 The d-electron methods

The widely know concept of designing Ti alloys which is referred to as the d-electron was first experimentally posed by Moringa *et al*. [23] and later by Kuroda *et al.* [3] with an objective of being a guideline when selecting alloying elements and the concept was also used to forecast of the phases are stable in alloys. The concept of d-electron is based on theoretical calculations of electronic structure of Ti alloys which is governed by a method called discrete-variational (DV) Xα cluster method [23]. Two parameters are widely reported in this method, and they are bond order (*Bo*) and the metal d-orbital energy level (*Md*) [24], where the *Bo* determines the strength of the covalent bonding that exist between atoms, it is reported that an increase in *Bo* value lead to a stronger chemical bond that exist between atoms. The second parameter is the *Md* which is associate with the electronegativity and metallic radius of elements. *Equation 1* below was used to determine the *Bo* and *Md* values of the studied alloy.

$$\overline{B_0} = \sum X_i (B_0)_i$$
$$\overline{M_d} = \sum X_i (M_d)_i \qquad \textbf{\textit{Equation 1}}$$

Where X_i represents atomic fraction of element *i* in an alloying element, (*Bo*)*i* and (*Md*)*i* are bond order and metal d-orbital energy level for element values of *i*, respectively [25], [26]. Morinaga *et al.* and Kuroda *et al.* have established a theoretical two-dimensional phase stability map which takes into considerations the electronic parameters that are established to be promising co-ordinates when designing and developing Ti alloys, [3], [27]. Vital information such as mechanical and chemical properties along with the type of deformation mechanism is demonstrated in the *Bo* and *Md* phase stability diagram. On the *Bo* and *Md* phase stability map, it is possible to predict phases that formed from quenching from high temperature and to estimate subsequent deformation mode since stress induced martensite phase transformation (TRIP), mechanical twinning (TWIP) and dislocation slip can exist depending upon on the stability of the β phase of the designed alloy. For example, the existence of dislocation slip takes place when an alloy exhibit higher β-phase stability, and mechanical twinning occurs at low β-phase stability, [24]. According to the phase stability map in Fig. ***1***, the calculated *Bo* and Md value of Ti-15Mo-2Fe alloy are mapped and demonstrated to be positioned in the slip region, this implies that the alloy will possesses dislocation slip as the most dominant deformation mechanism.

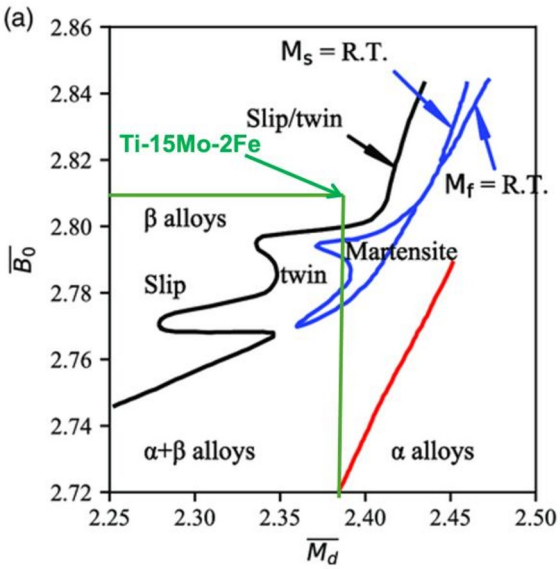

Fig. 1. Bo and Md phase stability map [24]

2.2 Molybdenum equivalence (Moeq)

The Molybdenum equivalence in wt.% (*Moeq*) is well documented method in literature that can be used to evaluate the stability of β phase. The team of Molchanova and Glazunov in 1965 [28], discovered and proposed the concept of *Moeq,* where the contribution of each alloying elements towards β phase stability is compared with Mo which is an effective stabilizer as opposed to other elements, [29]. A rough estimation of how the β phase will be stable or the deformation mechanism that a metastable β-Ti alloys might under can be given by *Moeq* method. A demonstration by Li *et al*., revealed that a metastable β-Ti alloys with *Moeq* value in the range of 9 to 16 wt.% undergo stress-induced β-α″ martensite transformation [29]. Suppression of deformation mechanisms such as transformation induced plastic (TRIP) and twinning induced plastic (TWIP) deformation mechanisms occurs when the *Moeq* increases, [29]. It is evaluated in literature that when the *Moeq* increases, the deformation modes changes from TRIP to TRIP/TWIP to TWIP and dislocation slip [30].

When the *Moeq* is reported to be under 10 wt.%, the deformation mechanism is dominated by TRIP, a range in the *Moeq* between 6 to 13 wt.% reveals a deformation mechanism of TRIP/TWIP and between 9 to 16 wt.%, TWIP is the predominant deformation mechanism. It was pointed that in the range between 7 and 16 wt.%, dislocation slip may become the most predominated deformation mechanism.

Complex elemental interaction that has the ability to influence the stability of β phase and the deformation mechanism in Ti alloys, such discrepancy may arise. Bania [10], developed the well-known formula for measuring the *Moeq*. Nevertheless, multiple elements such as Mo, Ta, Nd, Sn, Zr are incorporated to form ternary or quaternary alloy with an objective to stabilize the β phase. Thus, with their complex interaction, multiple elements show ability to alter the stability of β phase effect of each element. The presence of combination of multiple elements and the influence of β phase stability on elements such as Sn and Zr, the *Moeq* was modified in the following by Wang *et al*., [31]

$$[Moeq]^{(Wang)} = 1.0Mo + 1.25V + 0.59W + 0.28Nb + 0.22Ta + 1.93Fe + 1.84Cr + 1.50Cu + 2.46Ni + 2.67Co + 2.26Mn + 0.30Sn + 0.47Zr + 3.01Si - 1.47Al\ (\%wt). \qquad \textbf{Equation 2}$$

The calculated *Moeq* for Ti-15Mo-2Fe was recorded to be 18.86 wt.%, which was above the 16 wt.% and this predicted that the alloy would exhibit dislocation slip as the paramount deformation mechanism without the formation of other deformation mechanisms such as stress induced martensitic (SIM) or TRIP or TWIP. The deformation mechanism of Ti-15Mo-2Fe alloy predicted by *Moeq* is similar to the predictions made by the d-electron method

2.3 Materials preparation and fabrication process

Metastable β-type ternary Ti-Mo-Fe alloy, namely, Ti-15Mo-2Fe wt.% composition was explored in this study. High-purity metallic powders of titanium, molybdenum and iron were measured and cold compacted into green bodies using the Zwick-Roell testing machine. A maximum of 80 kN and crosshead speed of 20 mm/min are the parameters that were used during cold compaction. To further process the compacted green bodies, a rePowder Plasma melting system called AMAZEMET which is facilitated under high inert environment was used for melting process [32]. Argon gas was purged into the system, and this was to reduce the content of oxygen in the chamber to less than 100 ppm. The whole process of melting uses an arc with a current ranging from 70A to 270A to melt the powder compacts. The ingots were turned and re-melted at least 4 times on the water-cooled copper hearth to attain better homogeneity and the whole process was conducted without opening the melting chamber door. Most of metastable β-Ti alloys are not used in their as-cast state, but they are further processed either by heat treatment or thermo-mechanical techniques. Solution treatment was employed in this study, where the ingot was heated to higher temperature of 1100 ºC, held for an hour in that temperature and rapidly cooled by quenching into ice-brine.

2.4 Compression properties

Mechanical properties of as-quenched samples were examined using compression testing method. To determine how a material will respond when its under compression load is investigated using a compression test. The test includes measuring variables such as strain, stress and deformation of a material. Similar information that are acquired in tensile test are possible to be seen in the uniaxial compression test, because properties such as compression strength, strain ect can be determined. In this research study, ternary alloy was subjected to compression test at room temperature. Three rectangular shaped specimens with 4x4x8mm dimensions as shown in Fig. ***2*** were machined per alloy and tested following the ASTM E9 standard using an Instron™1342 machine under room temperature. Compression properties such as ultimate compression strength, compression yield strength and compression strain

were recorded. Micro-Vickers hardness of compressed samples was measured using the Zwick Roell hardness tester. The polished and etched surface was indented with a minimum of 10 indents under a 500gf load and 10 seconds dwell time.

Fig. 2. Rectangular shaped compression samples after wire cutting.

2.5 Phase and microstructural characterization

Phase and microstructural characterization of samples before and after compression were evaluated using various techniques such as X-ray diffractometer (XRD) and Optical microscope (OM). The phase analysis was carried out using the Malven Panalytical Empyrean diffractometer equipment. The Cu Kα radiation with the following parameters: secondary monochromatic (λ = 0.1545 nm) at 45 kV and 40 mA. The 2θ scan range is from 5° to 100 ° at a step size of 0.01°, were used to run the XRD Patterns. Specimens for optical micrographs were prepared succeeding the metallographic preparations techniques. To reveal the microstructure, Kroll reagent with the following concentrations: (90 ml H_2O, 2 ml HF, 3 ml HNO_3 and 5 ml HCl.) was used on the sample. OM micrographs were evaluated using the Leica optical microscope (OM).

3 Results

3.1 X-ray diffractometer

The phase constituent of Ti-15Mo-2Fe alloy before and after compression test was measured using the X-ray diffractometer (XRD) technique. As shown in Fig. ***3*** (a and b), the XRD patterns before and after compression depicted three phases: β phase, the orthorhombic martensitic phase (α″) and a newly reported trigonal rhombohedral (R) phase with a space group of R-3m. The "R" phase is attributed by the distortion of β phase prior to forming a trigonal omega phase [33]. The detection of the "R" phase is not yet widely reported in metastable β alloys however its 1st detection in Ti alloys was reported by [34] in ball milled and sintered pure Ti alloys. No other phases such as athermal omega phase (ω_{ath}) were detected in this alloy using the XRD characterization method. Earlier investigations by [35], [36] pointed out the existence of the athermal omega (ω_{ath}) phase from Ti-10Mo to Ti-20Mo alloys. However, according to Ref 11 and 37, ω_{ath} phase is difficult to detect by XRD since β and ω_{ath} phase peaks can overlap. Therefore, to distinguish the existence of the ω_{ath} phase in ternary alloys EBSD or TEM characterization techniques can be explored for future work.

The presence of the α″ phase in Ti-15Mo-2Fe contradicts the theoretical predictions that were made by the *Moeq* and the *Bo-Md* phase stability map: the *Moeq* calculated using an equation by Wang *et al.* that is used to determine the types of deformation mechanism that an alloy will exhibit, showed that since the alloy has a Moeq higher than 16 wt.% it will likely

possess dislocation slip as the dominant deformation [24]. The *Bo-Md* phase stability map also predicted similar results as it shows that the alloy is in the slip region. Martensitic transformation that occurs upon alloying or external load which results either in the formation of α″ or ω_{ath} phase occurs in metastable β Ti alloys which present a martensite start temperature below room temperature, [37], [38], [39] and this explains the presence of α″ phase before and after compression.

The discrepancies that occurred between the experimental data (especially those that consisted of non-equilibrium phases) and theoretical results could be attributed by several factors that are involved during processing of the alloys such as processing temperature, cooling medium, rate of cooling, deformation mechanism. These factors are not contemplated in theoretical methods. The presence of "R" phase that was seen in the XRD patterns could not be predicted by the predictive methods; thus, its existence could not be foreseen using the predictive methods. The experimental results of compressed Ti-15Mo-2Fe were found to be hard to compare to other literature work because the alloy is not widely explored after processing conditions such as solution treatment and compression test only. Thus, the alloy was compared to Ti-15Mo-1Fe reported by Min *et al.* after the alloy was rolled and tested for mechanical properties using tensile test method [15]. The authors reported the presence of β phase along with decreasing volume of (ω_{ath}) phase in their studied alloy. The XRD patterns of the studied ternary was different to XRD peaks of β phase only as-cast ternary Ti-xTa-xHf-xZr alloys after compression test which were reported by Lin *et al.* [18]. However, XRD patterns reported by Sadeghpour *et al.* showed almost similar patterns with the studied alloy in Ti-4Al-7Mo-3V-3Cr alloy [13]. XRD patterns of studied ternary alloys were dissimilar to XRD patterns in Ti-8Mo-2Fe, Ti-9Mo-1Fe and Ti-10.5Mo-1Fe alloys which were comprised of peaks belonging to both β and ω_{ath} phases [19].

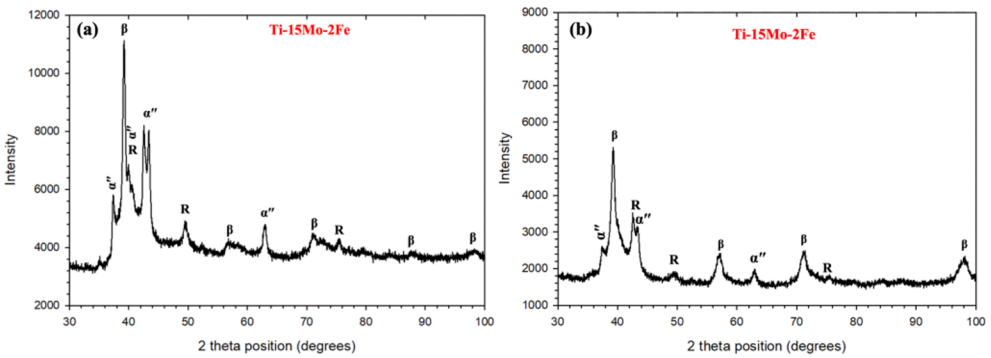

Fig. 3. XRD patterns of Ti-15Mo-2Fe alloy before compression (a) and after compression (b)

3.2 Optical micrographs

To investigate the microstructural constituents and deformation mode at low magnification, optical microscope was used to analyse the microstructure and deformation mode of Ti-15Mo-2Fe alloy before and after compression test at room temperature. Fig. ***4*** (a-d) respectively presents OM micrographs of Ti-15Mo-2Fe before and after compression. The OM micrographs of Ti-15Mo-2Fe alloy before and after compression test demonstrated large β equiaxed grains that were visible. The micrographs in Fig. ***4*** (a-b) did not show any other structures inside the large grains, however micrographs in Fig. ***4*** (c-d) they illustrated wide deformation bands and thin lines. According to literature, the wide bands are related to mechanical twins, and the thin lines are dislocation slip lines, [40]. These features are typical and complements characterization tools such as EBSD and TEM methods. Therefore, using the optical micrograph results, a premature conclusion can be deduced in Ti-15Mo-2Fe

micrograph that only β equiaxed grains are seen before compression and mechanical twins and slip are the occurring deformation mechanism after compression test.

Distinguishing the experimental results and the deformation mechanism that were forecasted using the theoretical methods, the following observations were deduced: The *Moeq* of Ti-15Mo-2Fe alloy was above 16 wt.% and this indicated that their predominant deformation mechanism will be comprised of dislocation slip only. The *Bo-Md* phase stability map method also predicted that the Ti-15Mo-2Fe alloy will be comprised of only dislocation slip as the only deformation mechanism. The optical micrographs were not agreeable with the theoretical results as the showed wide deformation bands that are correlated to mechanical twins. Both theoretical methods failed to foresee the presence of mechanical twining in all ternary alloys and this could be ascribed by the different parameters that are involved during processing of the alloys that are not considered when using theoretical methods. Due to less work reported in Ti-15Mo-2Fe alloy, the OM micrographs before compression were comparable to OM micrographs comprised of only β equiaxed grains which were reported by [19] in Ti-8Mo-2Fe, Ti-9Mo-1Fe and Ti-10.5Mo-1Fe alloys after several thermo-mechanical properties and the OM micrographs after compression test, were compared to several work in literature such as Ti-15Mo-1Fe alloy investigated by Min *et al*. [15], and alloys studied by Sadeghpour *et al.* in Ti-Al-Mo-V-Cr alloys [13].

. .

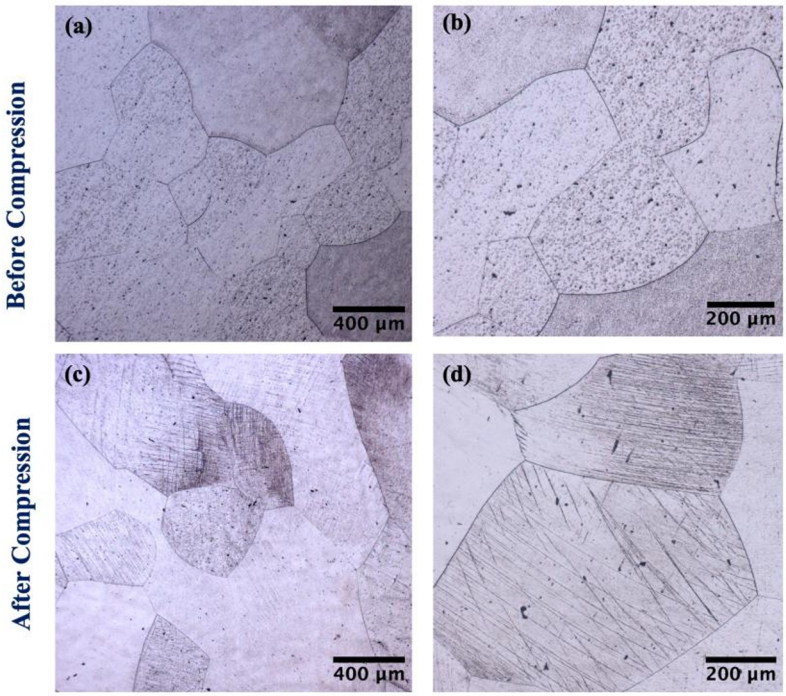

Fig. 4. Optical micrographs of Ti-15Mo-2Fe alloy before compression (a and b) and after compression test (c and d).

3.3 Compression properties

The ultimate compression strength of an alloy is the strength reached by an alloy before it can fracture. As part of the requirements for vascular stents, the strength should be high enough to resist fracturing. Hardness measures how hard the material or alloy is to avoid cracking during deformation. Strength and hardness of a material could be affected by

different factors such as the grain size, the deformation products, phases, processing techniques ect [41]. Yield strength of a material measures the stress in which the material can withstand before it can plastically deform [42]. Compression strain is a measure of deformation representing the decrease in the length of a material when it is subjected to compressive stress. High compression strain is required in vascular stents material because to ensure that they deform plastically, providing ductility and toughness that prevent brittle fracture. Compression properties such as ultimate strength, yield strength, compression strain and the Vickers hardness measured on the compressed samples are present in Table 1. An ultimate compression strength of 1522 MPa, the compression yield strength was recorded to be 1088 MPa, compression strain was 33% and Vickers hardness was 403 Hv.

The compression strength were found to be higher as opposed to ultimate tensile strength (UTS) of Ti-17Ir alloy (1448 MPa) that is designed for vascular stents [43] the studied alloy was also higher as opposed to metallic materials considered for vascular stents: Co-Cr alloy with UTS between 951-1220 MPa [44], stainless steel 586 MPa, Nitinol with 895 MPa [44], Ti-Ta alloy with UTS of 1151 MPa [43]. The high yield was lower as opposed to the alloys evaluated by Lin *et al.* in Ti-Ta-Hf-Zr alloys as seen in Table 1 [45], and this could be due to the presence of ω_{ath} phase that was reported by Lin *et al*. The yield strength of Ti-15Mo-2Fe was notably higher than metallic materials that are considered for vascular stents. It was noticeable that compression yield strength of Ti-15Mo-2Fe alloy was significantly higher as opposed to the tensile yield strength of Ti-15Mo-1Fe alloy evaluated by Min X *et al.* [15]. The compression strain of the ternary alloys were found to be lower to the compression strain of as-cast Ti-37Ta-26Hf-13Zr alloy which was investigated by Lin et al., (2016). Hardness of the studied alloy was higher as compared to that of the Ti-xTa-Hf-xZr alloys reported by Lin *et al.* [45], which could be due to the existence of stress-induced α″ phase that was not observed in Ti-xTa-Hf-xZr alloys. It is commonly known from literature that factors such as phase evolutions, microstructural features are the internal factors that determine the strength and hardness of a material, [46]. Microstructure is being regarded as the main factor as it includes the following four strengthening mechanisms which are solid solution strengthening, deformation strengthening, precipitation and dispersion strengthening, the other factor is grain and sub-grain strengthening, [18], [47]. Hence the high strength and hardness as opposed to other metallic materials might be due to the presence of stress-induced α″ phase and mechanical twinning deformation mechanism.

The high ultimate compression strength, compression yield strength and compression strain of the studied alloy showed great potential to be used in vascular stents application because of its high strength that surpasses those of other considered metallic materials. Due to direct relationship between hardness and wear, the high hardness value in Ti-15Mo-2Fe will results in excellent wear resistance, thus rendering this alloy suitable candidate for vascular stent applications.

Table 1. Compression properties of compressed Ti-15Mo-2Fe alloy.

Alloy Name (wt%)	**Ultimate compression strength (MPa)**	**Compression Yield strength (MPa)**	**Compression Strain (%)**	**Micro-Vickers Hardness (Hv)**	**References**
Ti-15Mo-2Fe	1522	1088	33	403	**This Study**
Ti-40Ta-22Hf-11.7Zr	-	1154	-	374.74	[18]
Ti-45Ta-18.4Hf-10Zr	-	1137	-	360.2	

Ti-37Ta-26Hf-13Zr	-	1158	34	380.88	
Ti-4Al-7Mo-3V-3Cr	-	875	35	-	
Ti-5Al-5Mo-5V-3Cr	-	830	30	-	
Co-Cr	951-1220	448-648		-	[48]
Stainless Steel	586	331	-	-	
Nitinol	895	195-690	-	-	

4 Conclusion

From work undertaken in this study, it can be summarized that the formation of α″ phase as revealed in the XRD patterns before and after compression was not expected according to the predictive methods used. Deformation products such as wide deformation bands that are associated with mechanical twinning and thin line associated with dislocation slip were noticeable after compression rest. The presence of high compression strength (both the ultimate compression and the compression yield) and high compression strain were attributed by the presence of wide deformation bands and dislocation slip. Hardness obtained was higher than that of the Ti6Al4V alloy. While there are few studies on the compression properties of Ti-15Mo-2Fe alloy, much improved mechanical properties were achieved in this study. The improvements might be attributed by the existence of orthorhombic martensitic phase (α″) and "R" phase as seen in the XRD graphs. The much-improved mechanical properties indicated that the alloy can be considered as a potential material for vascular stents applications.

The investigated study was supported financially by Mintek (Advance Materials Division) and the studies were supported by CSIR-IBS. The following institutions are recognized for their contribution with laboratory access: Mintek (AMD) and CSIR (AME and National Laser Center). The author extends gratitude to colleagues at Mintek (Mr Joseph Moema) for their immense support with experimental work.
Data Availability: The data that supports the findings of this study are obtainable from the following corresponding author: Moshokoa Nthabiseng, Maje Phasha and Elizabeth Makhatha

References

[1] Y. L. Hao, Z. B. Zhang, S. J. Li, and R. Yang, Microstructure and mechanical behavior of a Ti-24Nb-4Zr-8Sn alloy processed by warm swaging and warm rolling. Acta Mater. **60**, 2169–2177, (2012). https://doi.org/10.1016/j.actamat.2012.01.003

[2] J. Huang, Z. Wang, and K. Xue, Cyclic deformation response and micro mechanisms of Ti alloy Ti-5Al-5V-5Mo-3Cr-0.5Fe. Materials Science and Engineering: A. **528**, 8723–8732, (2011). https://doi.org/10.1016/j.msea.2011.08.045

[3] D. Kuroda, M. Niinomi, M. Morinaga, Y. Kato, and T. Yashiro, Design and mechanical properties of new i type titanium alloys for implant materials. Materials Science and Engineering A: **243**, 244-249, (1998). https://doi.org/10.1016/S0921-5093(97)00808-3

[4] E. Bertrand, P. Castany, I. Péron, and T. Gloriant, Twinning system selection in a metastable β-titanium alloy by Schmid factor analysis. Scr Mater. **64**, 1110–1113, (2011). https://doi.org/10.1016/j.scriptamat.2011.02.033

[5] A. Devaraj., V.V., Joshi, A., Srivastava, S., Manandhar, V., Moxson, V.A., Duz, and C., Lavender, A low-cost hierarchical nanostructured beta-titanium alloy with high strength. Nat Commun. **7**, 11176, (2016). https://doi.org/10.1038/ncomms11176

[6] S. Bahl, S. Suwas, and K. Chatterjee, Comprehensive review on alloy design, processing, and performance of β Titanium alloys as biomedical materials. International Materials Reviews. **66**, 114–139, (2021). https://doi.org/10.1080/09506608.2020.1735829

[7] M. Niinomi, M. Nakai, and J. Hieda, Development of new metallic alloys for biomedical applications. Acta Biomaterialia. **8**, 3888-3903, (2012). https://doi.org/10.1016/j.actbio.2012.06.037

[8] S. Ehtemam-Haghighi, Y. Liu, G. Cao, and L. C. Zhang, Phase transition, microstructural evolution and mechanical properties of Ti-Nb-Fe alloys induced by Fe addition. Mater Des. **97**, 279–286, (2016). https://doi.org/10.1016/j.matdes.2016.02.094

[9] M. Morinaga, Alloy design based on molecular orbital method. Materials Transactions. **57**, 213-226. (2016). https://doi.org/10.2320/matertrans.M2015418

[10] P. J. Bania, Beta Titanium Alloys and Their Role in the Titanium Industry. Jom, **46**, 16-19, (1994). https://doi.org/10.1007/BF03220742

[11] F. Sun., J.Y., Zhang, M., Marteleur, T., Gloriant, P., Vermaut, D., Laillé, P., Castany, C., Curfs, P.J., Jacques, and F.J.A.M., Prima, Investigation of early-stage deformation mechanisms in a metastable β titanium alloy showing combined twinning-induced plasticity and transformation-induced plasticity effects. Acta Mater. **61**, 6406–6417, (2013). https://doi.org/10.1016/j.actamat.2013.07.019

[12] A. Bhattacharjee, V. K. Varma, S. V Kamat, A. K. Gogia, and S. Bhargava, Influence of b Grain Size on Tensile Behavior and Ductile Fracture Toughness of Titanium Alloy Ti-10V-2Fe-3Al. Metall Mater Trans A. **37**, 1423–1433 (2006). https://doi.org/10.1007/s11661-006-0087-x

[13] S. Sadeghpour, S. M. Abbasi, M. Morakabati, A. Kisko, L. P. Karjalainen, and D. A. Porter, On the compressive deformation behavior of new beta titanium alloys designed by d-electron method. J Alloys Compd. **746**, 206–217, (2018). https://doi.org/10.1016/j.jallcom.2018.02.212

[14] L. Wang, W. Lu, J. Qin, F. Zhang, and D. Zhang, Microstructure and mechanical properties of cold-rolled TiNbTaZr biomedical β titanium alloy. Materials Science and Engineering: A. **490**, 421–426, (2008). https://doi.org/10.1016/j.msea.2008.03.003

[15] X. H. Min, T. Nishimura, S. Emura, N. Sekido, K. Tsuzaki, and K. Tsuchiya, Effects of Fe addition on tensile deformation mode and crevice corrosion resistance in Ti–15Mo alloy. Materials Science and Engineering: A. **527**, (2010). https://doi.org/10.1016/j.msea.2009.12.050

[16] A. G. Paradkar, S. V. Kamat, A. K. Gogia, and B. P. Kashyap, On the validity of Hall-Petch equation for single-phase β Ti-Al-Nb alloys undergoing stress-induced martensitic transformation. Materials Science and Engineering: A. **520**,168–173, (2009). https://doi.org/10.1016/j.msea.2009.05.041

[17] S. Hanada and O. Izumi, Transmission Electron Microscopic Observations of Mechanical Twinning in Metastable Beta Titanium Alloys. Metallurgical Transactions A. 17, 1409-1420, (1986). https://doi.org/10.1007/BF02650122

[18] J. Lin., S., Ozan, Y., Li, D., Ping, X., Tong, G. Li, and C., Wen, Novel Ti-Ta-Hf-Zr alloys with promising mechanical properties for prospective stent applications. Scientific Reports. **6**, 37901, (2016). https://doi.org/10.1038/srep37901

[19] C. Catanio Bortolan., L.C., Campanelli, P., Mengucci, G., Barucca, N., Giguère, N., Brodusch, C., Paternoster, C., Bolfarini, R., Gauvin, and D., Mantovani,

Development of Ti-Mo-Fe alloys combining different plastic deformation mechanisms for improved strength-ductility trade-off and high work hardening rate. J Alloys Compd. **925**, 166757, (2022). https://doi.org/10.1016/j.jallcom.2022.166757

[20] P. Castany, T. Gloriant, F. Sun, and F. Prima, Design of strain-transformable titanium alloys. Comptes Rendus. Physique. **19**, 710-720. (2018). https://doi.org/10.1016/j.crhy.2018.10.004

[21] M. Marteleur, F. Sun, T. Gloriant, P. Vermaut, P. J. Jacques, and F. Prima, On the design of new β-metastable titanium alloys with improved work hardening rate thanks to simultaneous TRIP and TWIP effects. Scr Mater. **66**, 749–752, (2012). https://doi.org/10.1016/j.scriptamat.2012.01.049

[22] F. Sun, F. Prima, and T. Gloriant, High-strength nanostructured Ti-12Mo alloy from ductile metastable beta state precursor. Materials Science and Engineering: A. **527**, 4262–4269, (2010). https://doi.org/10.1016/j.msea.2010.03.044

[23] M. Morinaga, N. Yukawa, and H. Adachi, Electronic Structure and Phase Stability of Titanium Alloys. *Tetsu-to-Hagane*, **72**, 555-562, (1986). https://doi.org/10.2355/tetsutohagane1955.72.6_555

[24] M. Abdel-Hady, K. Hinoshita, and M. Morinaga, General approach to phase stability and elastic properties of β-type Ti-alloys using electronic parameters. Scr Mater. **55**, 477–480, (2006). https://doi.org/10.1016/j.scriptamat.2006.04.022

[25] C. Li, D. G. Lee, X. Mi, W. Ye, S. Hui, and Y. Lee, Phase transformation and age hardening behavior of new Ti-9.2Mo-2Fe alloy. J Alloys Compd. **549**, 152–157, (2013). https://doi.org/10.1016/j.jallcom.2012.08.065

[26] M. Ahmed, D. Wexler, G. Casillas, O. M. Ivasishin, and E. V. Pereloma, The influence of β phase stability on deformation mode and compressive mechanical properties of Ti-10V-3Fe-3Al alloy. Acta Mater. 84, 124–135, (2015). https://doi.org/10.1016/j.actamat.2014.10.043

[27] M. Abdel-Hady, H. Fuwa, K. Hinoshita, H. Kimura, Y. Shinzato, and M. Morinaga, Phase stability changes with Zr content in β-type Ti-Nb alloys. Scr Mater. **57**, 1000–1003, (2007). https://doi.org/10.1016/j.scriptamat.2007.08.003

[28] E. K. Molchanoca and S. G. Glazunov, Phase diagrams of Titanium Alloys. Israel Program for scientific translations. (1965).

[29] C. Li, J. H. Chen, X. Wu, W. Wang, and S. Van Der Zwaag, Tuning the stress induced martensitic formation in titanium alloys by alloy design. J Mater Sci. **47**, 4093–4100, (2012). https://doi.org/10.1007/s10853-012-6263-z

[30] R. P. Kolli, W. J. Joost, and S. Ankem, Phase Stability and Stress-Induced Transformations in Beta Titanium Alloys. JOM. **67**, 1273-1280, (2015). https://doi.org/10.1007/s11837-015-1411-y

[31] Q. Wang, C. Dong, and P. K. Liaw, Structural Stabilities of β-Ti Alloys Studied Using a New Mo Equivalent Derived from [β/(α + β)] Phase-Boundary Slopes. Metall Mater Trans A Phys Metall Mater Sci. 46, 3440–3447, (2015). https://doi.org/10.1007/s11661-015-2923-3

[32] Ł. Żrodowski., R., Wróblewski, T., Choma, B., Morończyk, M., Ostrysz, M., Leonowicz, W., Łacisz, P., Błyskun, J.S., Wróbel, G., Cieślak, and B., Wysocki, Novel cold crucible ultrasonic atomization powder production method for 3d printing. Materials. **14**, 2541, (2021). https://doi.org/10.3390/ma14102541

[33] S. Banerjee, R. Tewari, and G. K. Dey, Omega phase transformation-morphologies and mechanisms. International Journal of Materials Research, **97**, 963-977, (2022).

[34] M. J. Phasha, A. S. Bolokang, and P. E. Ngoepe, Solid-state transformation in nanocrystalline Ti induced by ball milling. Mater Lett. **64**, 1215–1218, (2010). https://doi.org/10.1016/j.matlet.2010.02.054

[35] X. Zhao, M. Niinomi, M. Nakai, and J. Hieda, Beta type Ti-Mo alloys with changeable Young's modulus for spinal fixation applications. Acta Biomater. **8**, 1990–1997, (2012). https://doi.org/10.1016/j.actbio.2012.02.004

[36] M. Sabeena, S. Murugesan, P. Anees, E. Mohandas, and M. Vijayalakshmi, Crystal structure and bonding characteristics of transformation products of bcc β in Ti-Mo alloys. J Alloys Compd. **705**, 769–781, (2017). https://doi.org/10.1016/j.jallcom.2016.12.155

[37] M. Nakai, M. Niinomi, X. Zhao, and X. Zhao, Self-adjustment of Young's modulus in biomedical titanium alloys during orthopedic operation. Mater Lett. 65, 688–690, (2011). https://doi.org/10.1016/j.matlet.2010.11.006

[38] H. Matsumoto, S. Watanabe, and S. Hanada, Microstructures and mechanical properties of metastable β TiNbSn alloys cold rolled, and heat treated. J Alloys Compd. **439**, 146–155, (2007). https://doi.org/10.1016/j.jallcom.2006.08.267

[39] Y. Yang., S. Q. Wu, G. P. Li, Y. L. Li, Y. F. Lu, K. Yang, and P. Ge, Evolution of deformation mechanisms of Ti-22.4Nb-0.73Ta-2Zr-1.34O alloy during straining. Acta Mater. **58**, 2778–2787, (2010). https://doi.org/10.1016/j.actamat.2010.01.015

[40] X. H. Min, S. Emura, T. Nishimura, K. Tsuchiya, and K. Tsuzaki, Microstructure, tensile deformation mode and crevice corrosion resistance in Ti-10Mo-xFe alloys. Materials Science and Engineering: A. **527**, 5499–5506, (2010). https://doi.org/10.1016/j.msea.2010.06.016

[41] F. I. Jamhari., F.M., Foudzi, M.A., Buhairi, A.B., Sulong, N.A.M., Radzuan, N., Muhamad, I.F., Mohamed, N.H., Jamadon, and K.S., Tan, Influence of heat treatment parameters on microstructure and mechanical performance of titanium alloy in LPBF: A brief review. **24**, 4091-4110. (2023). https://doi.org/10.1016/j.jmrt.2023.04.090

[42] N. Saba, M. Jawaid, and M. T. H. Sultan, An overview of mechanical and physical testing of composite materials. In Mechanical and Physical Testing of Bio composites, Fibre-Reinforced Composites and Hybrid Composites. 1–12. https://doi.org/10.1016/B978-0-08-102292-4.00001-1

[43] B. O'Brien, J. Stinson, and W. Carroll, Initial exploration of Ti-Ta, Ti-Ta-Ir and Ti-Ir alloys: Candidate materials for coronary stents. Acta Biomater. **4**, 1553–1559, (2008). https://doi.org/10.1016/j.actbio.2008.03.002

[44] Davis J.R, Metallic Materials, Handbook of materials for medical devices. ASTM International. (2003).

[45] J. Lin., S., Ozan, Y., Li, D., Ping, X., Tong, G. Li, and C., Wen, Novel Ti-Ta-Hf-Zr alloys with promising mechanical properties for prospective stent applications. Scientific Reports. **6**, 37901, (2016). https://doi.org/10.1038/srep37901

[46] L. M. Kang and C. Yang, "A Review on High-Strength Titanium Alloys: Microstructure, Strengthening, and Properties. Advanced Engineering Materials. **21**, 1801359, (2019). https://doi.org/10.1002/adem.201801359

[47] L. Nie, Y. Zhan, H. Liu, and C. Tang, Novel β-type Zr-Mo-Ti alloys for biological hard tissue replacements. Mater Des. **53**, 8–12, (2014). https://doi.org/10.1016/j.matdes.2013.07.008

[48] Joon B. Park and Bronzino D Joseph, Biomaterials, 1st Edition. Boca Raton: CRC Press, 250 (2002). https://doi.org/10.1201/9781420040036